Single Image Orientation of UAV's Imagery Using Orthogonal Projection Model

Martinus Edwin Tjahjadi
Department of Geodesy
National Institute of Technology (ITN) Malang
Malang, Indonesia
edwin@lecturer.itn.ac.id

Fransisca Dwi Agustina
Department of Geodesy
National Institute of Technology (ITN) Malang
Malang, Indonesia
siscaagustina02@gmail.com

***Abstract*—A Perspective based image restitution for registering and processing UAV's images is widely known in photogrammetry and computer vision communities. Despite its reliability to compute all necessary parameters to model 3D objects, however it is less suitable to process images which have a very narrow angular field of view. An interested feature on images captured from a very distant imaging object or by a long focal length camera occupies a small portion of the field of view. The perspective model produces unstable results or singular outcomes if the image's field of view is less than 10 degrees. The captured ground features are usually located on small clusters which have very narrow field of view. Therefore, stable registration results are barely achieved. On the other hand, the orthogonal projection model was claimed to give stable results in such situation, particularly for a remote sensing imagery and a non-topographic photogrammetry. This paper demonstrates a feasibility of the orthogonal model based space resection to perform a featured based UAV image registration using surveyed ground control points. Using a minimum of 4 points to reach the field of view of around 6 degrees on each cluster, a five-group of collected clusters is computed. Whilst the perspective model produces erratic results, the orthogonal model gives better solution of exterior orientation parameters in all parts of the image.**

Keywords— Image processing; UAV; Resection; Orthogonal; Perspective; Projection

I. INTRODUCTION (*HEADING 1*)

Accurate registrations of images are fundamental prerequisites in aerial photogrammetry using Unmanned Aerial Vehicle (UAV) platform [1, 2]. Orientated images are necessary before commencing rigorous bundle adjustment [3] or image mosaicking processes [4]. Existing algorithmic approaches for image based registration (i.e. space resection method) which use a perspective projection model require that imaging cameras are within geometrically strong image networks [5]. For example, objects being measured on the image occupy an appropriate portion of the camera's angular Field of View (FoV). The perspective projection model is a standard photogrammetry method for processing aerial images and it is highly reliable to produce 3D models of ground features [3]. This imaging model achieves rigorous solutions by treating Euclidean space parameters (e.g. rotations and translations) as orientation parameters [6].

When the size of the portrayed objects become smaller on the image due to an increase of distances between ground surface objects and a mounted camera on the flying UAV, the angular FoV of the relevant portion of the resulting image decreases. The angular FoV becomes narrower and it makes a bundle of rays approach more parallel. If the FoV of the imaged objects is too narrow, it causes over parameterization in the perspective projection model (e.g. collinearity equation). As a result, numerical instability and near linear dependencies occur in the determination of interior orientation (IO) and exterior orientation (EO) parameters [7]. In this situation, the perspective projection model is hardly applicable due to ill-condition problems.

To circumvent this situation, computer vision methods reveal orthographic projections for modelling the imaging process [8-10]. The orthographic projection is categorized as the generalized affine model since its projective camera center is located at infinity [5]. These methods regard an invariant scale for establishing the image to object space correspondence. It rectifies perspective distortions within the narrow FoV area only. Although these models are stable in ill-condition infinity [5], algorithmic assumptions and variant camera geometries are absorbed into the homogeneous projective model which can also deteriorate the stability of the solutions.

On the other hand, Ono [6, 11] derived orthographic projection from the perspective model when the object size is small compare to the imaging distance from the camera to object. A bundle of rays emanating from the ground surface is conceived as a double projection. All of ground points are projected orthographically onto a so called "average plane" followed by a perspective projection onto the image plane under uniform scaling. Two constraints are imposed in the algorithm to enforce rays from the ground be orthogonal to the image plane and make an equal scale in the direction of image coordinate axes. This method is known as the orthogonal projection model. This model was claimed as accurate as the perspective projection model [7, 11].

Ministry of Research, Technology and Higher Education of the Republic Indonesia.

This paper demonstrates a usefulness of the orthogonal model compare against the perspective one in solving a single image orientation using space resection by utilizing Ground Control Points (GCPs). The GCPs are surveyed and observed using geodetic type Global Positioning System (GPS). They are distributed at a designed location, and are arranged in a sparse and cluster group of points. For an image registration process, the GCPs are portrayed during aerial photographing at a flying height of around 300m above the ground using a Sony Alpha-5100 camera with a fixed lens of 35mm. With its APS-C sensor size of 23.5mm x 15.6mm and 6000 x 4000 pixel format, it gives an angular field of view (FoV) of about 43.8^0 or about 3.5cm of Ground Sampling Distance (GSD).

A. Mathematical Projection Model

Conceptual illustrations of the perspective and orthogonal projection models are depicted in Fig.1 and Fig.2 respectively. A mathematical derivation of the orthogonal projection model is a scaled weak perspective projection of the ground surface features following by projective transformation into the central perspective images [11]. Let's start with the perspective projection model.

The following discussions are assumed that the principal points of pp(x_p, y_p) and the lens distortion be negligible. The ground coordinate system is a three dimensional right-handed Cartesian coordinate system whose orientation to the ground is defined by given coordinates $[X, Y, Z]^T$ (Fig.1). The camera or image coordinate system is also a three dimensional right-handed Cartesian coordinate system with the $[x, y]^T$ are being the image plane and the z axis being toward the perspective center O whose coordinates in the ground coordinate system is $[X_C, Y_C, Z_C]^T$. If c is the principal distance of the lens, the imaging process of the perspective projection model requires that the image vector $[x, y, -c]^T$ expressed in the camera coordinate system and the object vector $\begin{bmatrix} X-X_C & Y-Y_C & Z-Z_C \end{bmatrix}^T$ from the perspective center O to the ground point P expressed in the ground coordinate system are collinear (Fig.1).

It means that the components of two vectors expressed in the same coordinate system are equal, except for a scale factor λ. A multiplication of the object space vector by a rotation matrix **M** brings it into the image coordinate system as follows:

$$\begin{bmatrix} x \\ y \\ -c \end{bmatrix} = \lambda \mathbf{M} \begin{bmatrix} X-X_C \\ Y-Y_C \\ Z-Z_C \end{bmatrix} = \lambda \begin{bmatrix} m_{11} & m_{12} & m_{13} \\ m_{21} & m_{22} & m_{23} \\ m_{31} & m_{32} & m_{33} \end{bmatrix} \begin{bmatrix} X-X_C \\ Y-Y_C \\ Z-Z_C \end{bmatrix} \quad (1)$$

The matrix **M** describes the angular relationship between the ground and image coordinate systems in terms of a 3x3 orthogonal rotation matrix. Each element of the **M** is a cosine direction of an angle between each pair of coordinate axes; hence only three independent parameters determine the matrix. Common parameterization consists of sequential rotations in a specified order around the X, Y, Z axes. The angle ω is the rotation around the X axis, taken as positive in the direction that takes the +Y axis toward the +Z axis. The angle φ is the rotation about the once-rotated +Y axis taking the once-rotated +Z to the once-rotated +X axis. Meanwhile, the angle κ is the rotation about twice-rotated +Z axis taking the twice-rotated +X axis to the twice-rotated +Y axis. These matrices are multiplied together in a proper sequential order to give:

$$\begin{aligned} \mathbf{M} &= \mathbf{M}_\kappa \quad \mathbf{M}_\varphi \quad \mathbf{M}_\omega \\ m_{11} &= \cos\varphi\cos\kappa \\ m_{12} &= \sin\omega\sin\varphi\cos\kappa + \cos\omega\sin\kappa \\ m_{13} &= -\cos\omega\sin\varphi\cos o + \sin\omega\sin\kappa \\ m_{21} &= -\cos\varphi\sin\kappa \\ m_{22} &= -\sin\omega\sin\varphi\sin\kappa + \cos\omega\cos\kappa \\ m_{23} &= \cos\omega\sin\varphi\sin\kappa + \sin\omega\cos\kappa \\ m_{31} &= \sin\varphi \\ m_{32} &= -\sin\omega\cos\varphi \\ m_{33} &= \cos\omega\cos\varphi \end{aligned} \quad (2)$$

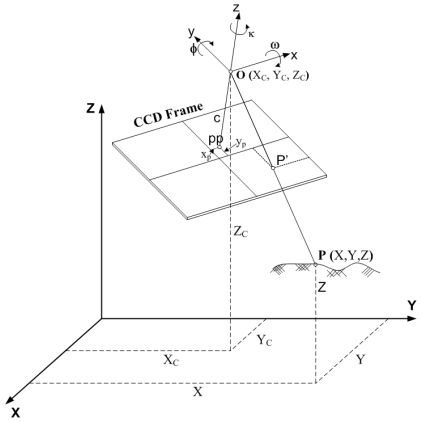

Fig. 1. A perspective projection model of a collinearity condition

The (1) yields three equations that describe the physical situation of the central perspective projection model's imaging process. If the first equation and the second equation are divided by third one and rearranging to yield a functional form, it gives the most commonly used of the collinearity equations:

$$x = x_p - c\left[\frac{m_{11}(X-X_C)+m_{12}(Y-Y_C)+m_{13}(Z-Z_C)}{m_{31}(X-X_C)+m_{32}(Y-Y_C)+m_{33}(Z-Z_C)}\right]$$
$$y = y_p - c\left[\frac{m_{21}(X-X_C)+m_{22}(Y-Y_C)+m_{23}(Z-Z_C)}{m_{31}(X-X_C)+m_{32}(Y-Y_C)+m_{33}(Z-Z_C)}\right] \quad (3)$$

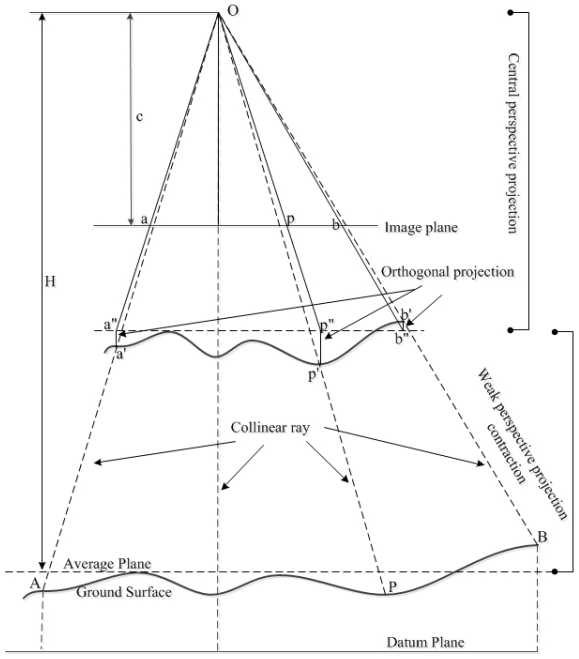

Fig. 2. An orthogonal projection model

The collinearity equations of (3) are utilized in photogrammetry to describe the perspective projection of ground points directly into their corresponding image. On the other hand, in the orthogonal projection model, a bundle of rays from ground points undergoes a transformation into a parallel rays (Fig.2). The weak perspective projection transform 3D ground points into an image plane by using 3D affine transformation with imposing constraints [11]. These constraints allow an oblique projection of rays become more parallel and perpendicular to the image plane. The scale factor λ in (1) is unknown scale value which varies for each object point. By substituting the λ by a constant scale parameter s, (1) can be rewritten as [11]:

$$\frac{s}{\lambda}\begin{bmatrix} x \\ y \\ -c \end{bmatrix} = \begin{bmatrix} x_a \\ y_a \\ -\frac{s}{\lambda}c \end{bmatrix} = s\begin{bmatrix} m_{11} & m_{12} & m_{13} \\ m_{21} & m_{22} & m_{23} \\ m_{31} & m_{32} & m_{33} \end{bmatrix}\begin{bmatrix} X-X_C \\ Y-Y_C \\ Z-Z_C \end{bmatrix} \quad (4)$$

By transposing $[X_C, Y_C, Z_C]$ to the left side, (4) can be recast as:

$$\begin{bmatrix} x_a - X'_C \\ y_a - Y'_C \\ -\frac{s}{\lambda}c - Z'_C \end{bmatrix} = s\begin{bmatrix} m_{11} & m_{12} & m_{13} \\ m_{21} & m_{22} & m_{23} \\ m_{31} & m_{32} & m_{33} \end{bmatrix}\begin{bmatrix} X \\ Y \\ Z \end{bmatrix} \quad (5)$$

Where:

$$\begin{bmatrix} X'_C \\ Y'_C \\ Z'_C \end{bmatrix} = -s\begin{bmatrix} m_{11} & m_{21} & m_{31} \\ m_{12} & m_{22} & m_{32} \\ m_{13} & m_{23} & m_{33} \end{bmatrix}\begin{bmatrix} X_C \\ Y_C \\ Z_C \end{bmatrix} \quad (6)$$

The first and second rows of (5) express the affine projection model [6, 11]as follows:

$$\begin{bmatrix} x_a \\ y_a \end{bmatrix} = s\begin{bmatrix} m_{11} & m_{12} & m_{13} \\ m_{21} & m_{22} & m_{23} \end{bmatrix}\begin{bmatrix} X \\ Y \\ Z \end{bmatrix} + \begin{bmatrix} X'_C \\ Y'_C \end{bmatrix} \quad (7)$$

The scale *s* is an arbitrary constant and (x_a, y_a) are called affine image coordinates. Practically, it is adjusted so as to scale down the average imaging distance to be the same length as the principal distance c, as per Fig.2. In a simplified form, (7) can be recast as the affine projection model:

$$\begin{aligned} x_a &= A_1X + A_2Y + A_3Z + A_4 \\ y_a &= A_5X + A_6Y + A_7Z + A_8 \end{aligned} \quad (8)$$

The (8) has eight degrees of freedom (dof) and it allows oblique projection to an image plane, but a perpendicularity of rays from the ground and image plane is not guaranteed, also the scale *s* in the x_a and y_a direction is not equivalent. Addition of constraint of (8) leads to the orthogonal projection model. Since the parameters A_i are derived from the component of rotation matrix m_{ij} and the scale parameter s, they should have the following properties of an orthogonal rotation matrix [6]:

$$\begin{aligned} A_1A_5 + A_2A_6 + A_3A_7 &= 0 \\ A_1^2 + A_2^2 + A_3^2 &= A_5^2 + A_6^2 + A_7^2 \end{aligned} \quad (9)$$

The first constraint of (9) implies that the dot product of vectors $\vec{r}_x = [A_1 \quad A_2 \quad A_3]^T$ and $\vec{r}_y = [A_5 \quad A_6 \quad A_7]^T$ has to be zero. This enforces incident rays from the ground to be orthogonal to the image plane. The second constraint implies that the norm of $\vec{r}_x$ and $\vec{r}_y$ must be equal. It means that the scale of x_a direction is equivalent to that in the y_a direction. These constraints reduce the dof of (8) from 8 to 6 in the orthogonal projection model and enable a uniform scale factor for the principal distance and for the projection center to the ground along the optical axis [7].

II. RESEARCH METHODOLOGY

To work with the orthogonal projection model, an initial conversion from observed central perspective image coordinates (x, y) to an affine projection image coordinates (x_a, y_a) is necessary. This step is as follows. Let H be the average photographing distance (Fig.2) in the Z direction. If $\overline{Z}$ is an elevation of the average plane, i.e. $H = \overline{Z} - Z_C$, an equal proportion between the average photographic distance and the principal distance would be:

$$s = -m_{33}\, c / \overline{Z} - Z_C = -m_{33}\, c / H \tag{10}$$

A third row of the reverse transformation of (1) can be used to calculate λ of every image point as follows:

$$\lambda = m_{13}\, x + m_{23}\, y - m_{33}\, c / Z - Z_C \tag{11}$$

By substituting (10) and (11) into (1), the expressions from transforming perspective projection image coordinates to orthogonal projection image coordinates are solved as:

$$\begin{aligned} x_a &= \left(\frac{Z - Z_C}{H}\right)\frac{m_{33}\, c}{m_{33}\, c - m_{13}\, x - m_{23}\, y}\, x \\ y_a &= \left(\frac{Z - Z_C}{H}\right)\frac{m_{33}\, c}{m_{33}\, c - m_{13}\, x - m_{23}\, y}\, y \end{aligned} \tag{12}$$

The m_{ij} are the element of the rotation matrix that can be calculated by a four points method [12] or by a three points method [13]. Before calculating the parameters of the orthogonal projection model, the affine model's parameter must be computed first. A mathematical model of a linear least squares adjustment of (8) is calculated as follows:

$$\begin{aligned} \begin{bmatrix} x_{a1} \\ x_{a2} \\ \vdots \\ x_{an} \end{bmatrix} &= \begin{bmatrix} X_1 & Y_1 & Z_1 & 1 \\ X_2 & Y_2 & Z_2 & 1 \\ \vdots & \vdots & \vdots & \vdots \\ X_n & Y_n & Z_n & 1 \end{bmatrix} \begin{bmatrix} A_1 \\ A_2 \\ A_3 \\ A_4 \end{bmatrix} \\ \begin{bmatrix} y_{a1} \\ y_{a2} \\ \vdots \\ y_{an} \end{bmatrix} &= \begin{bmatrix} X_1 & Y_1 & Z_1 & 1 \\ X_2 & Y_2 & Z_2 & 1 \\ \vdots & \vdots & \vdots & \vdots \\ X_n & Y_n & Z_n & 1 \end{bmatrix} \begin{bmatrix} A_5 \\ A_6 \\ A_7 \\ A_8 \end{bmatrix} \end{aligned} \tag{13}$$

Equation (13) are of the form $\boldsymbol{L} = \boldsymbol{BX}$ and have the least squares solutions $\boldsymbol{X} = (\boldsymbol{B}^T\boldsymbol{B})^{-1}\,(\boldsymbol{B}^T\boldsymbol{L})$. n is the number of the GCP, and the minimum numbers of GCP to uniquely solve the parameter for image (A_1, …, A_8) are four points. By solving these two equations, initial approximations for the affine projection parameters are obtained.

Then, to enforce orthogonal constraints among the affine parameters, they are readjusted by applying constraints of (9). The Helmert's bordering method [14, 15] is chosen to constraint the least squares solution:

$$\begin{bmatrix} \mathbf{N} & \mathbf{H}^T \\ \mathbf{H} & \mathbf{0} \end{bmatrix} \begin{bmatrix} \boldsymbol{\delta} \\ \mathbf{k_h} \end{bmatrix} = \begin{bmatrix} \mathbf{c} \\ \mathbf{w_h} \end{bmatrix} \tag{14}$$

The **H** is a 2x8 matrix of additional constraints, $\boldsymbol{\delta}$ is a 8x1 correction vector of the parameter, $\mathbf{w_h}$ is the discrepancy vector of the constrain equation, $\mathbf{k_h}$ is a multiplier vector which is out of interest of the present discussion. The normal equation matrix of **N** and the vector **c** are constituted from:

$${}_{2n}\mathbf{B}_8 = \begin{bmatrix} X & Y & Z & 1 & 0 & 0 & 0 & 0 \\ 0 & 0 & 0 & 0 & X & Y & Z & 1 \end{bmatrix} \tag{15}$$

The matrix **H** is formed based on (9) as follows:

$${}_2\mathbf{H}_8 = \begin{bmatrix} A_5 & A_6 & A_7 & 0 & A_1 & A_2 & A_3 & 0 \\ 2A_1 & 2A_2 & 2A_3 & 0 & -2A_5 & -2A_6 & -2A_7 & 0 \end{bmatrix} \tag{16}$$

The last step of the process is the conversion process of the orthogonal projection model's parameters into the EO parameters which constitutes three rotations of Euler angles (ω, φ, κ) and a position of the perspective center (X_C, Y_C, Z_C). From (7) and (9) it is known that

$$\begin{bmatrix} A_1 & A_2 & A_3 \\ A_5 & A_6 & A_7 \end{bmatrix} = s \begin{bmatrix} m_{11} & m_{12} & m_{13} \\ m_{21} & m_{22} & m_{23} \end{bmatrix} \tag{17}$$

The rest of the rotation matrix elements can be obtained as follows

$$\begin{aligned} &m_{31} = \pm\sqrt{1 - m_{11}^2 - m_{21}^2};\; m_{32} = \pm\sqrt{1 - m_{12}^2 - m_{22}^2}; \\ &m_{33} = \pm\sqrt{1 - m_{13}^2 - m_{23}^2} \end{aligned} \tag{18}$$

The final values of rotational element can be derived by (2). The position of the perspective center is derived as

$$\begin{aligned} Z_C &= {}^{m_{33}\, c}\!\diagup_{s} + \overline{Z} \\ Y_C &= \frac{A_1A_8 - A_4A_5 - A_3A_5Z_C + A_1A_7Z_C}{A_2A_5 - A_1A_6} \\ X_C &= -\left(A_4 + A_2Y_C + A_3Z_C\right)/A_1 \end{aligned} \tag{19}$$

The $\overline{Z}$ is averaged elevations of the GCP's ground coordinate system.

III. Results and Discussion

Two field observations were carried out in Malang city. An array of 50 GCPs is established and measured using three units of geodetic type GPS instrument. Each GCP is observed around 20 minutes and all points give an accuracy of about 2mm (Fig. 3). A white concentric ring surrounded with dark background [16] is selected and set up on the field (Fig. 4) to facilitate a possible highest accuracy of image coordinate measurements of GCPs on images.

Fig. 3. Rapid static GPS measuremt on the GCP

Fig. 4. Some of GCPs on the field

The GCPs were imaged using aforementioned camera, and one of the results is shown in Fig. 5. To simulate a very narrow FoV, 5 clusters of the GCPs are created. Each cluster consists of 4 points of which give a unique solution of the space resection of the perspective projection model.

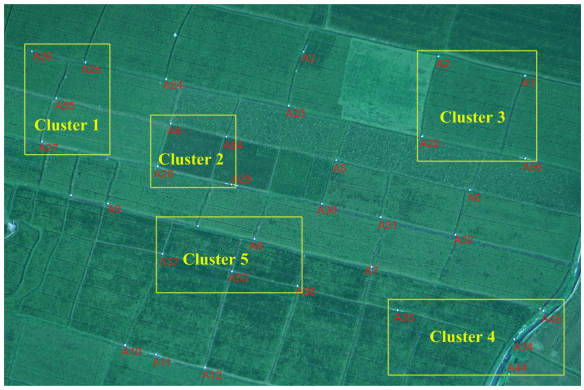

Fig. 5. Distribution of the 33 photographed GCPs.

As a true value of the EO parameters, the rigorous projection model's space resection is performed utilizing all 33 GCPs (Table 1). These values are set as a benchmark against the ones that of computed using the perspective and orthogonal projection model on each cluster area.

TABLE I. A benchmark of the EO Parameters

EO parameter	Value	Standard Error (1 Sigma)
Omega - ω (deg)	-2.6368	0.01162
Phi - φ (deg)	3.9069	0.01633
Kappa - κ (deg)	88.933	0.00203
X_C (m)	679421.0695	0.07492
Y_C (m)	9123785.2218	0.05419
Z_C (m)	794.8981	0.01085

Table II and Table III show the EO parameters computed on each cluster using 4 GCPs. Table II compares the result of rotational elements of the EO using the orthogonal model against the perspective one. The orthogonal model produces more stable results than that of the perspective model. The erratic result of the perspective model is based on the fact that each cluster has the FoV around 6 degrees. Hence, a bundle of rays emanating from these GCP becomes more parallel when reaching the image plane. As a result, the rotation elements from the perspective model are less stable, particularly for omega and phi rotation angles.

TABLE II. Rotation Elements of EO Parameters from the Orthogonal and Perspective Projection Model

	Orthogonal Projection Model			**Perspective Projection Model**		
	ω^o	φ^o	κ^o	ω^o	φ^o	κ^o
Cluster 1	-2.6368	3.9068	88.935	-4.4668	4.9957	89.025
Cluster 2	-2.6379	3.9107	88.933	-4.7718	1.6182	89.217
Cluster 3	-2.6268	3.9062	88.928	-1.8381	4.481	89.037
Cluster 4	-2.6136	3.9066	88.931	-0.4763	1.3743	88.748
Cluster 5	-2.6403	3.9019	88.930	-1.4296	-2.6826	88.755

TABLE III. Position Elements of EO Parameters from the Orthogonal and Perspective Projection Model

	Orthogonal Projection Model			Perspective Projection Model		
	X_C (m) 679…	Y_C (m) 9123…	Z_C (m)	X_C (m) 679…	Y_C (m) 9123…	Z_C (m)
Cluster 1	421.446	785.460	800.630	425.859	793.413	790.991
Cluster 2	421.248	785.322	797.138	410.428	794.708	792.101
Cluster 3	421.022	785.187	794.080	423.539	781.722	793.019
Cluster 4	420.678	784.958	789.375	409.653	775.558	791.549
Cluster 5	421.024	785.203	794.323	391.125	779.803	794.032

Meanwhile, Table III shows a comparison of the perspective center camera resulted from the orthogonal and perspective model computation. Following to the rotation elements, more stable result occurs from the orthogonal model. The largest difference of the X_C, Y_C, Z_C in the perspective model when compared to the benchmark values are around 30, 10, and 4 meters respectively; however, the result of the same criteria for the orthogonal model are only 0.5, 0.3, and 6 meters respectively. In contrast, higher discrepancies of Z_Cs in the Z direction of the orthogonal model are due to a dimensional reduction in the affine projection model from 3D to 2D model. Overall, these facts demonstrate that the orthogonal projection model produce more accurate and stable result of computing the EO parameters when using features which occupy only small part of the image.

IV. Conclusion

This paper demonstrates a feasibility of the orthogonal model based space resection to perform a featured based UAV image registration using surveyed ground control points. While the perspective model produces erratic results, the orthogonal model gives better solution of exterior orientation parameters in all clusters on the image. It is clearly show that the orthogonal projection model is well suited to compute the EO parameters from only small part of the UAV's image, particularly when the FoV is less than 6 degrees. This method would be useful for UAV's image registration using features which not largely spanned.

Acknowledgment

The author wishes to express his sincere thanks to Ministry of Research, Technology and Higher Education of the Republic of Indonesia for supporting a research grant "Penelitian Terapan Unggulan Perguruan Tinggi (PTUPT)", with an announcement letter number 025/E3/2017 and a contract number 073/SP2H/K2/KM/2017 and ITN.05.071.03 /I.LPPM/2017.

References

[1] M. Saadatseresht, A. H. Hashempour, and M. Hasanlou, "UAV Photogrametry: a Practical Solution for Challenging Mapping Projects," The International Archives of the Photogrammetry, Remote Sensing and Spatial Information Sciences, vol. XL(1/W5), pp. 619-623, 2015.

[2] Y. Zhang, J. Z. Li, P. P. Jiang, Y. L. Du, and S. F. Gong, "Using Image Registration Method to Register UAV," Applied Mechanics and Materials, vol. 716(717), pp. 1675-1679, Dec 2014.

[3] T. Anai, T. Sasaki, H. Otani, K. Osaragi, and N. Kochi, "Aerial photogrammetry procedure optimized for micro uav," The International Archives of the Photogrammetry, Remote Sensing and Spatial Information Sciences, vol. XL(5), pp. 41-46, June 2014.

[4] M. E. Tjahjadi, F. Handoko, and S. S. Sai, "Novel Image Mosaicking of UAV's Imagery Using Collinearity Condition," International Journal of Electrical and Computer Engineering (IJECE), vol. 7(3), pp. 1188-1196, June 2017.

[5] M. Rova, S. Robson, and M. Cooper, "Multistation Bundle Adjustment with a Machine Vision Parallel Camera System-an Alternative to the Perspective Case for the Measurement of Small Objects," The International Archives of Photogrammetry and Remote Sensing and Spatial Information Sciences, vol. 37(B5), pp. 45-50, 2008.

[6] T. Ono and S. Hattori, "Fundamental Principles of Image Orientation Using Orthogonal Projection Model," The International Archives of Photogrammetry and Remote Sensing, vol. 34(3/B), pp. 194-199, 2002.

[7] C. Stamatopoulos and C. S. Fraser, "An orthogonal projection model for photogrammetric orientation of long focal length imagery," Proceeding of AfricaGEO, 2011.

[8] B. K. Ghosh and E. Loucks, "A perspective theory for motion and shape estimation in machine vision," SIAM Journal on Control and Optimization, vol. 33(5), pp. 1530-1559, 1995.

[9] T. S. Huang and C. Lee, "Motion and structure from orthographic projections," IEEE Transactions on Pattern Analysis and Machine Intelligence, vol. 11(5), pp. 536-540, 1989.

[10] X. Hu and N. Ahuja, "Motion estimation under orthographic projection," IEEE Transactions on Robotics and Automation, vol. 7(6), pp. 848-853, 1991.

[11] T. Ono, S.. Akamatsu, and S. Hattori, "A Long Range Photogrammetric Method with Orthogonal Projection Model,"The International Archives of Photogrammetry and Remote Sensing, vol. 35(3), pp. 1010-1015, 2004.

[12] S. Kyle, "Using Parallel Projection Mathematics to Orient an Object Relative to a Single Image," Photogrammetric Record, vol. 19(105), pp. 38-50, March 2004.

[13] M. E. Tjahjadi, "A Fast And Stable Orientation Solution of Three Cameras-Based UAV Imageries," ARPN Journal of Engineering and Applied Sciences, vol. 11(5), pp. 3449-3455, 2016.

[14] E. M. Mikhail, "Parameters Constraints in Least Squares," Photogrammetric Engineering, vol. 36(12), pp. 1277-1291, 1970.

[15] H. Wolf, "The Helmert Block Method - Its Origin and Development," in International Symposium on Problems Related to the Redefinition of North American Geodetic Networks, Arlington, Virginia, pp. 319-326, 1978.

[16] T. Clarke and X. Wang, "Extracting high-precision information from CCD images," in Proc. ImechE Conf., Optical methods and data processing for heat and fluid flow, City University, pp. 311-320, 1998.